

## Electric field control of magnetic exchange coupling

K. Leistner<sup>1,2\*</sup>, J. Wunderwald<sup>1,2</sup>, N. Lange<sup>1,2</sup>, S. Oswald<sup>1</sup>, M. Richter<sup>1</sup>, H. Zhang<sup>1,3</sup>, L. Schultz<sup>1,2</sup>, S. Fähler<sup>1</sup>

<sup>1</sup>IFW Dresden, P.O. Box 270116, D-01171 Dresden, Germany.

<sup>2</sup>Faculty of Mechanical Engineering, Institute for Materials Science, Dresden University of Technology, D-01062 Dresden, Germany.

<sup>3</sup>Forschungszentrum Jülich GmbH, D-52425 Jülich, Germany.

\*Correspondence to: k.leistner@ifw-dresden.de

**Abstract:** Electric control of magnetism is a vision which drives intense research on magnetic semiconductors and multiferroics. Recently, also ultrathin metallic films were reported to show magnetoelectric effects at room temperature. Here we demonstrate much stronger effects by exploiting phase changes in a naturally grown oxide layer exchange coupled to an underlying ferromagnet. For the exemplarily studied FePt/iron oxide composite in an electrolyte, a large and reversible change of magnetic moment and anisotropy is obtained. The principle can be transferred to various metal/oxide combinations. It represents a novel approach towards multifunctional materials.

**One Sentence Summary:** Electric field control of magnetic exchange coupling exponentiates the application potential of nanoscale magnetoelectric composites.

**Main Text:** Though the interdependence of magnetism and electricity had already been described by Maxwell in 1861, it took more than a century until it was realized that the coupling between magnetic and electric polarization in solid matter may exponentiate the application potential of polarized materials. To date there are two main material classes exhibiting magnetoelectric effects: magnetic semiconductors (1) and insulating multiferroics (2). Both utilize the weak coupling of their intrinsic bulk polarization. This constraint leaves application above room temperature an open challenge. Two-phase multiferroics consisting of ferromagnetic/ferroelectric composites (3) overcome this limitation. Since (ferro-) elastic coupling mediates between both phases, they however cannot be applied in microsystems where thin composite films are clamped by thick, rigid substrates. Thus, alternative approaches are sought to address the growing demand on multifunctional nanosystems. For example benefit can be drawn from the increased surface to volume ratio at the nanoscale. This idea expands the range of applicable materials towards metals with a thickness of just a few nanometers. In the bulk of metals, the free electrons shield any electric field. This does not hold for the surface atomic layers. Accordingly, electric fields can be used to change the mechanical properties of metallic nanoparticles (4, 5), to control magnetocrystalline anisotropy, coercivity and Curie temperature in ultrathin films (6-9) and to induce surface phase changes (10). In combination with the spin torque effect (11) or the precession of magnetization (12), the electric field dependence of the magnetocrystalline anisotropy even allows bistable magnetization switching (13). Huge effects are obtained when Curie temperature coincides with application temperature (6-9).

Here, we investigate ultrathin ferromagnetic metallic films with the advantage of a high Curie temperature. This avoids unfavorable cross-correlations originating from the high temperature dependency of magnetocrystalline anisotropy close to Curie temperature. First we show how a critical point can be adjusted in a metallic layer, which allows toggling between two magnetic states; second we demonstrate how the electric field can be used to switch between two magnetic phases in a naturally grown oxide layer. The electric field is applied by the established approach of electrochemical charging (4, 6). This allows understanding changes in both, magnetic anisotropy and moment by means of electrochemical concepts.

In order to prepare a critical situation between two magnetic states, we used the competition between two independent contributions to magnetic anisotropy. The high aspect ratio of film thickness vs. lateral extension results in a large shape anisotropy preferring a magnetization direction within the film plane to reduce magnetic stray field energy. As an antagonist, the intrinsic magnetocrystalline anisotropy was used which favors magnetization along specific crystallographic directions. In order to align these crystallographic directions, we took advantage of the strong influence of the interface by epitaxial growth. We tuned the relation between shape and magnetocrystalline anisotropy in 2 nm thick FePt films by varying the annealing time  $t_A$  (Figure 1). At a given annealing temperature,  $t_A$  determines the degree of order, which is essential for the strength of magnetocrystalline anisotropy in this system (14).

The  $t_A$ -dependent transition from an in-plane to an out-of-plane magnetization can be followed in magnetization measurements based on the anomalous Hall effect. We selected this method as it is sensitive enough for ultrathin films and compatible with the electrochemical charging applied later. The magnetic field was oriented perpendicular to the film plane. Hence, for films with in-plane magnetization, increasing field results in a continuous rotation out-of-plane visible in an almost linear increase of the Hall signal in Figure 1. Without annealing ( $t_A = 0$  min), saturation is reached at 1.4 T which is precisely the anisotropy field expected for a disordered A1 FePt thin film with a saturation magnetization of 1.4 T and negligible magnetocrystalline anisotropy. Applying post annealing leads to steeper curves showing reduced in-plane total anisotropy. This can be explained by a continuous increase of magnetocrystalline anisotropy due to increasing  $L1_0$  chemical order. For  $t_A = 15$  min, the Hall signal reveals a step-like switching, reflecting a magnetization process along an easy axis. Saturation is achieved in low fields by domain wall motion.

In order to quantify the transition from in-plane ( $t_A = 0$ ) to out-of-plane ( $t_A = 15$  min) anisotropy one can use the area between magnetization curve, magnetization axis and saturation magnetization (inset in Figure 2B). This area defines an effective anisotropy constant  $K_{\text{eff}}$ . To obtain a large reversible variation of  $K_{\text{eff}}$  by an electric field we used films annealed for an intermediate time ( $t_A = 5$  min) and charged them in an electrolyte. In contrast to previous work of Weisheit et al. (6) who charged FePt in a Na/PC electrolyte under ambient atmosphere, we used  $\text{LiPF}_6$  solved in DMC/EC and placed the complete assembly in an argon box. As described in detail in (16) this method allowed to use an expanded potential window between Fe dissolution and electrolyte side reactions from 2 to 3 V vs.  $\text{Li/Li}^+$ .

The magnetic behavior of a typical film charged between 2 and 3 V is depicted in Figure 2. We observe a strong dependence of the maximum anomalous Hall resistance  $R_{AH,S}$ , which is taken as a measure of the saturation magnetization, on the applied potential, Figure 2A. Repeated charging experiments (I to IV in the inset of Figure 2A) proof that this change in saturation magnetization is reversible. At the same time, a reversible change in the shape of the

magnetization curve is observed, see Figure 2B. At 3 V, the curve is steeper and reaches saturation at lower magnetic fields than at 2 V. This finding indicates a decrease of out-of-plane magnetocrystalline anisotropy for negative charging (addition of electrons).

To quantify the effect, we consider  $K_{\text{eff}}$  and normalize it to its value measured at 3 V:  $\Delta K = 1 - K_{\text{eff}}/K_{\text{eff}}(3 \text{ V})$ . The potential dependences of  $\Delta K$  and of an equivalently defined  $\Delta R_{AH}$  in saturation are summarized in Figure 3. Anticipating further analysis, our data are referred to as FePt/Fe-O. If the potential is reduced from 3 to 2 V, the effective anisotropy decreases by 25% while the magnetization increases by 4%.

At this point we can state an astonishingly strong electric-field dependence of magnetic properties, achieved by tuning ultrathin metallic films to a point of almost compensating anisotropies. We find a relative change of the anisotropy which is *one order of magnitude larger* than in previous experiments (6). In addition, we observe a variation of saturation magnetization similar to results on CoPd films and nanoparticles (17, 18).

As an attempt to explain the observed 4% increase of magnetization when adding about  $0.2 e^-$  per surface atom, we performed density-functional calculations using the procedure described in (19). These calculations describe the effect of band filling by the additional surface charge. They yield a marginal decrease of magnetization ( $-0.25\%$  for  $0.1 e^-$  addition) instead of a substantial increase. This inconsistency indicates that filling of the FePt bands cannot be the essential mechanism behind the measured effect.

In the following, we present experimental evidence that electric field control of metallic magnetism can be achieved by induced phase changes in an exchange coupled composite. We show that this new mechanism can explain the variation of both quantities, anisotropy and magnetization. For this aim, we investigated the surface condition of our films in more detail. As in previous experiments (6, 18), the films had been handled under ambient conditions between growth and measurements. Though FePt is commonly considered as inert due to the noble metal component, exposure to air may result in the formation of a thin natural iron oxide. Indeed, X-ray photo emission spectroscopy (XPS) (Figure 4A) reveals a partial but significant shift of the Fe  $2p_{3/2}$  peak toward the position expected for iron oxides. Accordingly, we refer to these samples as FePt/Fe-O composites. As a cross check, we investigated samples directly transferred into the Ar-box to avoid oxidation. As no peak shift is observed in XPS in this case (Figure 4B), we denote these samples single phase FePt. When repeating the electric field experiments for a single phase FePt sample, only minor variations of magnetization and anisotropy are observed (Figure 3A and B). Hence, the large variations observed for the FePt/Fe-O samples have to be attributed to the presence of iron oxide and not to an electronic band filling of the metallic FePt.

Electrochemical concepts based on redox reactions in this iron oxide surface film can be used for explanation. Phase changes in iron oxides and hydroxides occur in the following order for negative charging in aqueous solution (20):  $\text{FeO}_x(\text{OH})_{3-2x}$ , FeOOH, and  $\text{Fe}_2\text{O}_3$  are subsequently reduced to  $\text{Fe}_3\text{O}_4$  and, at even lower potentials, finally to Fe. The oxidized species ( $\text{FeO}_x(\text{OH})_{(3-2)x}$ , FeOOH, and  $\text{Fe}_2\text{O}_3$ ) are non-magnetic or weakly ferromagnetic, while the reduced species ( $\text{Fe}_3\text{O}_4$  and Fe) are ferrimagnetic and ferromagnetic with a saturation polarization of 0.6 T and 2.1 T, respectively. For surface-near regions these reduction processes can be reversible and subsequent anodic charging again oxidizes the surface to  $\text{Fe}_3\text{O}_4$  and FeOOH (20). Thus, a charge-induced phase change from a non-magnetic iron oxide surface layer to a ferri- or ferro-

magnetic surface layer can well explain the observed reversible increase of saturation magnetization for negative charging.

In aqueous solution, protons are involved in the reduction reaction (e.g.  $\text{Fe}_3\text{O}_4 + 8 \text{H}^+ + 8 \text{e}^- \leftrightarrow 3 \text{Fe}^0 + 4 \text{H}_2\text{O}$ ) (20). In the present nonaqueous Li-based electrolyte protons are not available, but  $\text{Li}^+$  ions can take their part. This mechanism was e. g. reported for the reduction/oxidation of transition metal nanoparticles in 1 M  $\text{LiPF}_6$  in DMC/EC (21). There, a lithium-driven reversible oxidation/reduction reaction has been described for cobalt oxide according to:  $\text{CoO} + 2 \text{Li}^+ + 2 \text{e}^- \leftrightarrow \text{Li}_2\text{O} + \text{Co}$ . We propose that a similar oxidation/reduction of iron oxide is responsible for the observed reversible change of magnetic moment. The current-voltage curve in Figure 3C does not show distinct reaction peaks, but rather an open rectangular double-layer-like behavior without any peaks. However, a kinetic analysis by scan rate dependent measurements (inset in Figure 3C) reveals that the voltammetric charge is proportional to the square root of rate. This behavior is expected for pseudocapacitance in metal oxides where several reduction steps overlap each other (22). In this case the modification of oxidation state is coupled to rate determining ion exchange processes (23). This situation differs from double layer charging which should be almost rate independent. Hence, the measured rate dependence excludes pure band filling without phase change.

The phase change in the surface iron oxide layer contributes significantly to the overall magnetization because ultrathin FePt films are used. In addition, the anisotropy of the composite is strongly affected. The concept of exchange coupling between hard and soft phases can well explain the observed decrease of the out-of-plane contribution to the anisotropy at negative potential. Exchange coupling of hard and soft magnetic phases significantly reduces the effective anisotropy in comparison to the isolated hard magnetic phase. This has been exploited irreversibly already for hard magnetic FePt nanocomposites coupled to soft magnetic Fe (25) or iron oxide phases (26). For a complete coupling the extension of the soft magnetic layer (in our case the reduced phases  $\text{Fe}_3\text{O}_4$  and Fe) must be shorter than the exchange length, which is in the order of 5 nm for FePt. This is easily achieved here, as the thickness of the natural surface iron oxide on our films must per se be smaller than the overall film thickness of 2 nm. This means that the soft magnetic magnetite or Fe layer forming at negative charges is fully exchanged coupled to the underlying FePt and thus results in the observed decrease of anisotropy.

To conclude, we demonstrated that electric field control of magnetism is possible on the basis of phase changes in metal oxides. For this goal, ultrathin composite films are of benefit in two ways: (1) they allow adjusting a critical point between shape and magnetocrystalline anisotropy and (2) they result in a complete exchange coupling in magnetic hard/soft composites. By the charge-induced change between surface phases with different magnetic properties, a variation of anisotropy by 25% is obtained, compared to 5% by pure electrical charging of FePt thin films (6). Our electrochemical analysis reveals that  $E$ -field induced variations of saturation magnetization can be attributed to oxidation/reduction processes. We suggest examining the relevance of this mechanism also on previous experiments (6, 17) since sometimes experiment and explanation by electron theory differ by sign (8, 18). Similar redox processes are involved during resistive switching of thin oxide layers, a novel route for nonvolatile storage (27). Hence our approach is not limited to electrochemical charging and can be extended to various metal/oxide combinations allowing tailoring magnetoelectric properties. In particular magnetic data storage can benefit from our approach. Reducing coercivity to facilitate the writing

processes is an urgent need, but approaches like thermally assisted magnetic recording require substantial technological efforts (28).

### References and Notes:

1. D. Chiba, M. Yamanouchi, F. Matsukura, H. Ohno, Electrical Manipulation of Magnetization Reversal in a Ferromagnetic Semiconductor. *Science* **301**, 943 (2003).
2. T. Lottermoser, T. Lonkai, U. Amann, D. Hohlwein, J. Ihringer, M. Fiebig, Magnetic phase control by an electric field. *Nature* **430**, 541 (2004).
3. H. Zheng *et al.*, Multiferroic BaTiO<sub>3</sub>-CoFe<sub>2</sub>O<sub>4</sub> Nanostructures. *Science* **303**, 661 (2004).
4. J. Weissmüller, R. N. Viswanath, D. Kramer, P. Zimmer, R. Wüschum, H. Gleiter, Charge-Induced Reversible Strain in a Metal. *Science* **300**, 312 (2003).
5. H.-J. Jin, J. Weissmüller, A Material with Electrically Tunable Strength and Flow Stress. *Science* **332**, 1179 (2011).
6. M. Weisheit, S. Fähler, A. Marty, Y. Souche, C. Poinignon, D. Givord, Electric Field-Induced Modification of Magnetism in Thin-Film Ferromagnets. *Science* **315**, 349 (2007).
7. T. Maruyama *et al.*, Large voltage-induced magnetic anisotropy change in a few atomic layers of iron. *Nature Nanotech.* **4**, 158 (2009).
8. D. Chiba, S. Fukami, K. Shimamura, N. Ishiwata, K. Kobayashi, T. Ono, Electrical control of the ferromagnetic phase transition in cobalt at room temperature. *Nature Mater.* **10**, 853 (2011).
9. F. Bonell *et al.*, Large change in perpendicular magnetic anisotropy induced by an electric field in FePd ultrathin films. *Appl. Phys. Lett.* **98**, 232510 (2011).
10. L. Gerhard *et al.*, Magnetoelectric coupling at metal surfaces. *Nature Nanotech.* **5**, 792 (2010).
11. W.-G. Wang, M. Li, S. Hageman, C. L. Chien, Electric-field-assisted switching in magnetic tunnel junctions. *Nature Mater.* **11**, 64 (2012).
12. Y. Shiota *et al.*, Induction of coherent magnetization switching in a few atomic layers of FeCo using voltage pulses. *Nature Mater.* **11**, 39 (2012).
13. E. Y. Tsymlal, Electric toggling of magnets. *Nature Mater.* **11**, 12 (2012).
14. F. Kurth *et al.*, Finite-size effects in highly ordered ultrathin FePt films. *Phys. Rev. B* **82**, 184404 (2010).
15. T. Shima, K. Takanashi, Y. K. Takahashi, K. Hono, Coercivity exceeding 100 kOe in epitaxially grown FePt sputtered films. *Appl. Phys. Lett.* **85**, 2571 (2004).
16. K. Leistner *et al.* Electrode processes and in-situ magnetic measurements of FePt films in an LiPF<sub>6</sub> electrolyte, submitted to *Electrochim. Acta*, preprint attached as supplementary material (2011).
17. S. Gosh, C. Lemier, J. Weissmüller, Charge-Dependent Magnetization in Nanoporous Pd-Co Alloys. *IEEE Trans. Magn.* **42**, 3617 (2006).

18. M. Zhernenkov, M. R. Fitzsimmons, J. Chlistunoff, J. Majewski, Electric field modification of magnetism in a thin CoPd film. *Phys. Rev. B* **82**, 024420 (2010).
19. H. Zhang, M. Richter, K. Koepf, I. Opahle, F. Tasnadi, H. Eschrig, Electric-field control of surface magnetic anisotropy: a density functional approach. *New J. Phys.* **11**, 043007 (2009).
20. G. V. M. Jacintho, P. Corio, J. C. Rubim, Surface-enhanced Raman spectra of magnetic nanoparticles adsorbed on a silver electrode. *J. Electroanal. Chem.* **603**, 27 (2007).
21. P. Poizot, S. Laruelle, S. Grugeon, L. Dupont, J.-M. Tarascon, Nano-sized transition-metal oxides as negative-electrode materials for lithium-ion batteries. *Nature* **407**, 496 (2000).
22. B. E. Conway, *Electrochemical Supercapacitors* (Kluwer Academic/Plenum Publishers New York, Boston, Dordrecht, London, Moscow, 1999) pp. 286.
23. S. Ardizzone, G. Fregonara, S. Trasatti, Inner and outer active surface of RuO<sub>2</sub> electrodes. *Electrochim. Acta* **35**, 263 (1990).
24. N. de Sousa *et al.*, Spin configurations in hard/soft coupled bilayer systems: Transitions from rigid magnet to exchange-spring. *Phys. Rev. B* **82**, 104433 (2010).
25. A. Breitling, T. Bublat, D. Goll, Exchange-coupled L1<sub>0</sub>-FePt/Fe composite patterns with perpendicular magnetization. *Phys. Stat. Sol. RRL* **3**, 130 (2009).
26. D. Hinzke, U. Nowak, R. W. Chantrell, O. N. Mryasov, Orientation and temperature dependence of domain wall properties in FePt. *Appl. Phys. Lett.* **90**, 082507 (2007).
27. R. Waser, M. Aono, Nanoionics-based resistive switching memories. *Nature Mater.* **6**, 833 (2007).
28. B. C. Stipe *et al.*, Magnetic recording at 1.5 Pbm<sup>-2</sup> using an integrated plasmonic antenna, *Nat. Photonics* **4**, 484 (2010).

**Acknowledgements:** We acknowledge H. Schlörb for discussion. This work is funded by DFG by project LE2558/1-1.

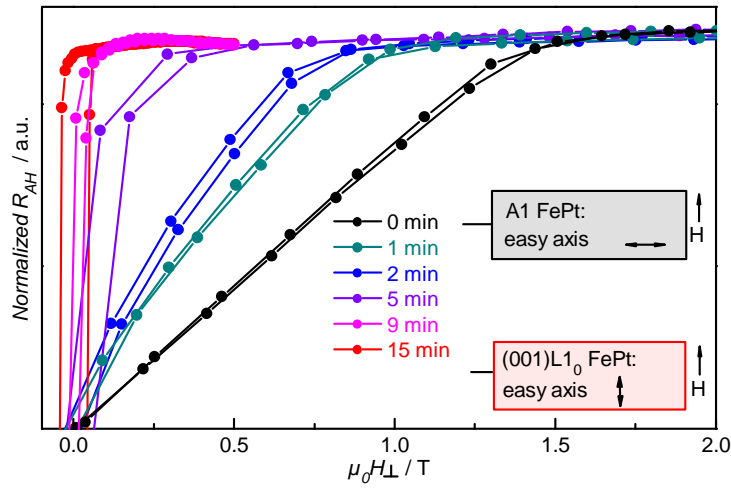


**Fig. 1.** Tuning the relation between shape and magnetocrystalline anisotropy. The graph shows the first quadrant of magnetization curves measured by the anomalous Hall effect with the field applied perpendicular to the substrate. By increasing the annealing times  $t_A$  from 0 to 15 min at 450°C the magnetization curves become gradually steeper and the easy axis changes from in-plane to out-of-plane. This is explained by an increase of magnetocrystalline anisotropy originating from a continuous change from A1 to L<sub>10</sub> chemical order in 2 nm thick FePt films (sketched in the inset).

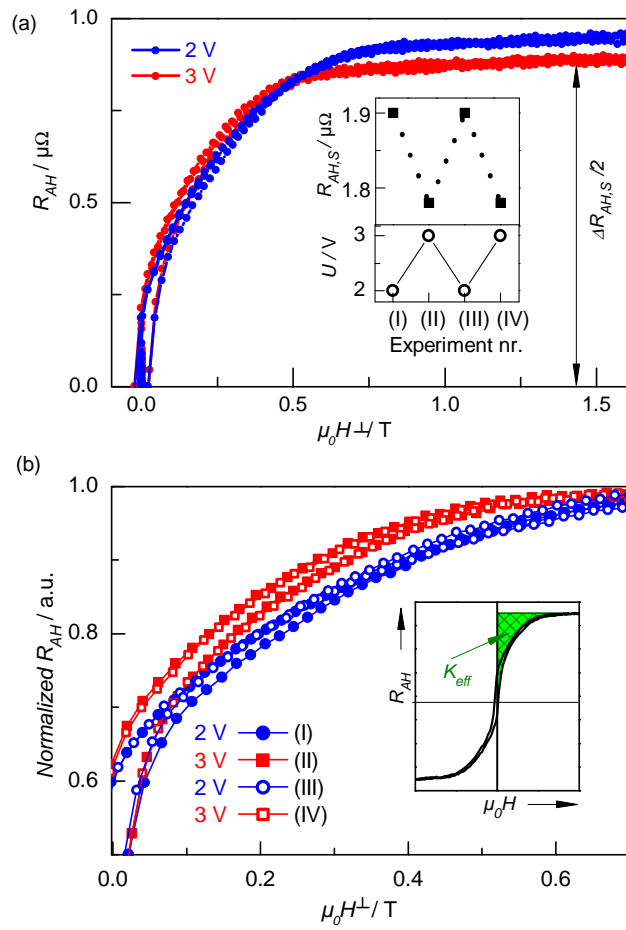


**Fig. 2.** Reversible change of magnetism by an electric field. a) The first quadrant of magnetization curves as probed by the anomalous Hall effect is shown for an FePt film ( $t_A = 5$  min) at applied potentials of 2 and 3 V. The inset demonstrates reversibility of the effect by comparing the maximum Hall voltage  $R_{AH,S}$  as a measure for the saturation magnetization obtained in a sequence of experiments (I to IV). b) Normalized curves revealing the reversibility of the curvature change. The inset illustrates the applied definition of the effective anisotropy  $K_{eff}$ .

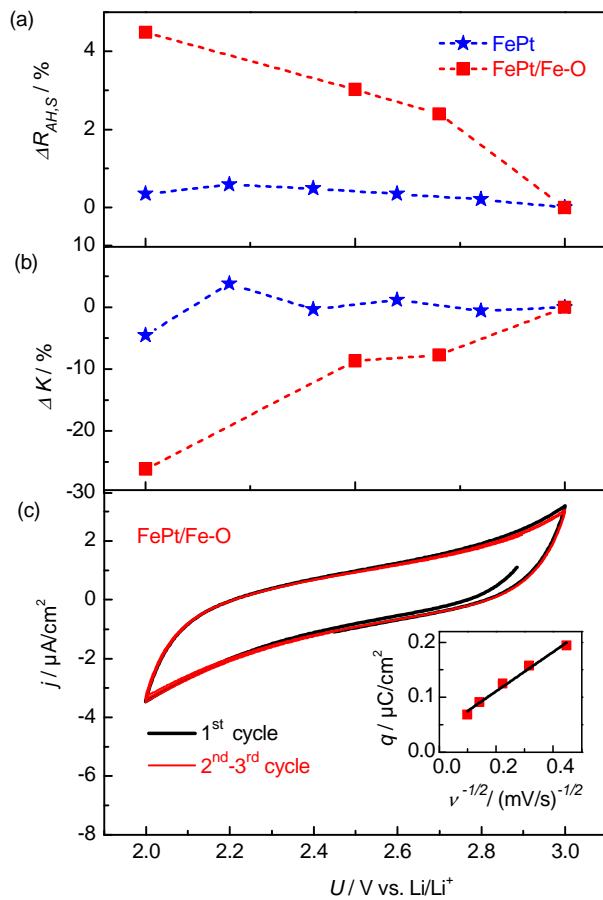


**Fig. 3.** Influence of electric field on magnetism for a composite FePt/Fe-O and for a single phase FePt sample. a) Change of  $R_{AH}$  as a measure for the change of saturation magnetization, b)  $\Delta K$  versus applied voltage; c) Corresponding current–voltage curve of the FePt/Fe-O composite film (scan rate 5 mV/s) and voltammetric charge  $q$  versus reciprocal square root of the scan rate  $v$ .

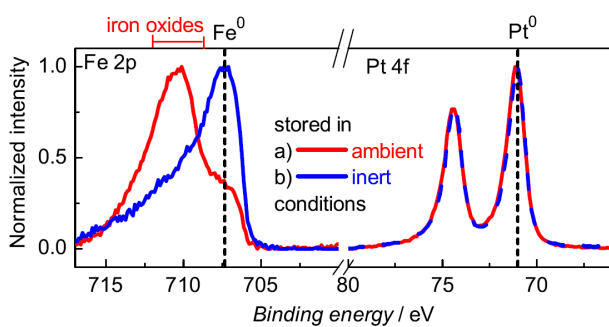


**Fig. 4.** Fe 2p<sub>3/2</sub> and Pt 4f<sub>5/2,7/2</sub> XPS spectra for 2 nm FePt films stored under a) ambient conditions and b) Ar atmosphere.

## Supplementary Materials:

### Materials and Methods

2 nm FePt thin films were grown by pulsed laser deposition on heated MgO(001) substrates with 3 nm Cr and 50 nm Pt buffer layers.  $L1_0$  ordering results in a tetragonal distortion of the unit cell, hence this buffer can be used to align the magnetically easy  $c$ -axis out-of-plane (6). The conducting thick buffer layers allowed for the use of the films as electrodes in an electrochemical cell. Cr and Pt were deposited at a substrate temperature of 300°C. The FePt films were deposited from a FePt alloy target at 450°C. During post annealing the films remained in the substrate heater and temperature was held constant for times between 0 and 15 min. In the present films coercivity values are low compared to granular  $L1_0$  films, as in our continuous films reverse domains can easily switch the whole film once they are nucleated at a defect (15).

For ultrathin films, conventional magnetometry is hampered by the low overall magnetization and impossible for a sample in an electrolytic cell. Therefore, anomalous Hall effect measurements were used instead. In Hall geometry, the magnetic field was applied perpendicular to the film plane. The Hall resistivity  $R_{Hall}$  for ferromagnets is the sum of ordinary ( $R_0$ ) and anomalous ( $R_{AH} = R_S M(H)$ ) terms:  $R_{Hall} = R_0 H + R_{AH}$ . Hystereses presented here are corrected for the normal Hall effect, obtained by the linear increase at high magnetic fields. A current between 10 and 100 mA was applied along one in-plane direction and the Hall voltage was measured along the other in-plane direction. Thus, the magnetization component perpendicular to the film plane was probed. The Hall measurements proved to be reliable, as identical hysteresis loops were obtained by measurements of the magneto-optical Kerr effect in the polar configuration.

For electrochemical charging, a nonaqueous electrolyte composed of 0.1 M  $LiPF_6$  in DMC/EC (1:1) was used. The charge per surface atom was calculated from the current-voltage curves in a three electrode cell and assuming an FePt(001) surface with Pt termination. For in-situ Hall measurements, an electrochemical cell compatible with a Physical Properties Measurement System (PPMS) system was constructed. As counter electrode, Li connected to a Cu wire was used, and the electrolyte was filled in a compartment sealed with O-rings. Electrical contacts were realized by press contacts on the sample outside the electrolyte compartment. The in-situ Hall cell was assembled in an Ar-Box to avoid air contamination of the electrolyte. Films were charged between 2 and 3 V vs.  $Li/Li^+$ . These upper and lower potential limits were determined in preceding electrochemical experiments (16) in order to avoid Fe dissolution and electrolyte side reactions.

The chemical states of Pt and Fe were investigated by means of X-ray photoelectron spectroscopy. The measurements were carried out at a PHI 5600 CI (Physical Electronics) spectrometer which is equipped with a hemispherical analyser operated with a typical pass energy of 29 eV and an analysis area of 800  $\mu m$  diameter. Monochromatic Al-K excitation (350 W) was used.

**Author contributions:** KL coached the experiments, understood the underlying mechanism and wrote the paper. JW performed the experiments to establish the critical point. NL designed the in situ cell and performed the in situ experiments. SO made the XPS measurements. MR contributed with discussion and formulation of the manuscript. HZ performed DFT calculations. LS supervised the experimental work. SF had the ideas and contributed to writing.